Anatomical predictors of successful prism adaptation in chronic visual neglect

Marine Lunven, PhD[1,2,3,4,5], Gilles Rode, MD, PhD[3,6], Clémence Bourlon, PhD[2,7], Christophe Duret MD[2], Raffaella Migliaccio, MD, PhD[1], Emmanuel Chevrillon, MD[8], Michel Thiebaut de Schotten, PhD[1,4*], Paolo Bartolomeo, MD, PhD[1*].

1. *Inserm U 1127, CNRS UMR 7225, Sorbonne Université, UPMC Univ Paris 06 UMR S 1127, Institut du Cerveau et de la Moelle épinière, ICM, Hôpital de la Pitié-Salpêtrière, F-75013, Paris, France.*
2. *Service de Médecine Physique et Réadaptation, Unité de Rééducation Neurologique CRF "Les Trois Soleils" Boissise le Roi, France*
3. *Inserm UMR_S 1028, CNRS UMR 5292; ImpAct, centre des neurosciences de Lyon, université Lyon-1, 16, avenue Lépine 69676 Bron, France*
4. *Brain connectivity and behaviour group, Sorbonne Université, Paris France.*
5. *Laboratoire de Neuropsychologie Interventionnelle, Département d'études cognitives, ENS, PSL Research University, UPEC, Université Paris-Est, CNRS, Paris France*
6. *Service de médecine physique et réadaptation neurologique, hôpital Henry-Gabrielle, hospices civils de Lyon, 20, route de Vourles, Saint-Genis-Laval, France*
7. *Hôpitaux de Saint Maurice, Saint Maurice, France*
8. *Clinique du Bourget, Le Bourget, France*

*contributed equally

Corresponding author: Paolo Bartolomeo, paolo.bartolomeo@gmail.com
ICM – Hôpital Pitié Salpêtrière, PICNIC Lab, 47, Bd de l'Hôpital, 75013 Paris – France
+33 (0)1 57 27 40 00

Cover title: Anatomical predictors of neglect rehabilitation

Key words: visual spatial neglect, prism adaptation, cortical thickness, white matter disconnection

Subject Terms: Cognitive impairment, Rehabilitation, Magnetic Resonance Imaging (MRI)

Character count for title: 78 characters
Word count: 5557
Number of references: 45
Number of tables: 5
Number of figures: 3

Abstract

Background and Purpose. To assess the hypothesis that prism adaptation improves left neglect after right brain damage by facilitating compensation through the contribution of the left, undamaged hemisphere. **Methods**. We assessed the relationship between prism adaptation effects, cortical thickness and white matter integrity in a group of 14 patients with unilateral right-hemisphere strokes and chronic visual neglect. **Results.** Patients who benefitted from prism adaptation had thicker cortex in temporo-parietal, prefrontal and cingulate areas of the left, undamaged hemisphere. Additionally, these patients had a higher microstructural integrity in the body and genu of the corpus callosum. Results from normal controls show that these callosal regions connect temporo-parietal, sensorimotor and prefrontal areas. Finally, shorter time intervals from the stroke tended to improve patients' response to prism adaptation. **Conclusions**. Prism adaptation appears to improve left visual neglect by promoting the contribution of the left hemisphere to neglect compensation. These results support current hypotheses on the role of the healthy hemisphere in the compensation for stroke-induced, chronic neuropsychological deficits, and suggest that prism adaptation can foster this role by exploiting sensorimotor/prefrontal circuits, especially when applied at early stages post-stroke.

1. Introduction

A major challenge of precision medicine is to relate individual patients' characteristics to their clinical outcomes. Patients with right hemisphere damage and left visual neglect are unable to pay attention to left-sided objects, with consequent loss of autonomy and poor functional outcome [1]. At least 80% of patients with a right hemispheric stroke show signs of visual neglect in the acute stage [2]. Impaired integration of attention-related processes within the right hemisphere [3,4], as well as between the hemispheres [5], contributes to neglect behavior. About half of neglect patients still show signs of neglect one year or more after their stroke [6], perhaps because posterior callosal dysfunction prevents attention-critical regions in the healthy hemisphere to access information processed by the damaged right hemisphere [6].

Prism adaptation (PA) is a convenient technique to improve the ratio of recovering patients because it is totally non-invasive and easy to administer [7,8]. Prismatic goggles displace the whole visual field rightwards and induce an initial rightward bias in manual reaching movements, which disappears after a few trials. After removal of the prisms, reaching initially deviates towards the left neglected side, and neglect eventually disappears. Unfortunately, neglect does not improve in all treated patients [9–12], for unknown reasons [13].

Drawing on our previous evidence suggesting a role for posterior callosal dysfunction in the chronic persistence of neglect [6], we hypothesized that PA might improve neglect by facilitating compensation through the contribution of the left, undamaged hemisphere. To test this hypothesis, we assessed the relationship between PA effects, cortical thickness and white matter integrity by following up a group of 14 patients with unilateral right-hemisphere stroke and chronic left visual neglect.

2. Methods

2.1. Standard Protocol Approvals, Registrations, and Patient Consents

The study was promoted by the Inserm (C10-48) and approved by the Ile-de-France I Ethics Committee (2011-juin-12642). All participants gave written informed consent to participate in the study.

2.2. Subjects

A group of 14 patients with a single right hemisphere hemorrhagic or ischemic stroke, which had occurred at least 3 months before testing, showing stable signs of left visual neglect. None of the patients had a prior history of neurological disease or psychiatric disorders. Table 1 reports patients' demographic, clinical and neuropsychological data. Visual neglect was assessed by using six paper-and-pencil tasks: letter cancellation [1] , copy of a linear drawing of a landscape [14] , drawing from memory of a daisy; text reading [2] , bisection of five 20-cm horizontal lines [2] and landmark task [15] . All patients performed these tests on three occasions: (1) the day before PA, (2) two hours before PA, and (3) soon after PA. For each assessment, a neglect severity score was computed as previously reported [6] , by using the percentage of left omissions for letter cancellation, drawing and reading tasks, the percentage of rightwards deviation for line bisection, and the percentage of left lateralised errors for the landmark task. Ten age-matched healthy subjects (mean age, 62.8 years; SD, 4.54; Mann-Whitney-Wilcoxon test, p ns) served as controls for neuroimaging.

2.3. Prism adaptation

Following a previously described procedure [8] , patients were asked to wear prismatic goggles that shifted the visual field 10 degrees towards the right. While wearing prisms, patients were required to make, as quickly as possible, a series of approximately 100 pointing responses with the right hand towards left and right targets. The starting point of the hand was occluded to ensure optimal adaptation. The head of the patients was aligned with their body sagittal axis. Patients were eye-blinded and asked to point ten times straight-ahead with their right arm before

and after the PA. Recovery scores were defined as the percentage of neglect improvement after PA using the following formula: (neglect score post-PA – neglect score pre-PA) / (neglect severity score pre-PA). We adopted an arbitrary cutoff of 20% change, which is often used in clinical studies [16] , to divide patients into two groups according to their recovery score. Patients with a recovery score above 20% were attributed to the "high-responder" group (N=8), whereas patients with a recovery score below 20% were considered as "low-responders" (N=6). This classification was in good agreement with the clinical assessment of neglect (see Table 1).

2.4. Imaging data acquisition and lesion analysis

2.4.1. Data acquisition

An axial three-dimensional MPRAGE dataset covering the whole head was acquired for each participant (176 slices, voxel resolution = 1 × 1 × 1 mm, TE = 3 msec, TR = 2300 msec, flip angle = 9°) on a Siemens 3 T VERIO TIM system equipped with a 32-channel head coil.

Additionally, a total of 70 near-axial slices was acquired using an acquisition sequence fully optimized for tractography of DWI, which provided isotropic (2 × 2 × 2 mm) resolution and coverage of the whole head. The acquisition was peripherally-gated to the cardiac cycle with an echo time (TE) = 85 msec. We used a repetition time (TR) equivalent to 24 RR intervals assuming that spins would have fully relaxed before the repetition. At each slice location, six images were acquired with no diffusion gradient applied. Additionally, 60 diffusion-weighted images were acquired, in which gradient directions were uniformly distributed in space. The diffusion weighting was equal to a b-value of 1500 sec mm^{-2}. One supplementary image with no diffusion gradient applied but with reversed phase-encode blips was collected. This provides us with a pair of images with no diffusion gradient applied with distortions going in opposite directions. From these pairs the susceptibility-induced off-resonance field was estimated using

a method similar to that described in [17] and corrected on the whole diffusion weighted dataset using the tool TOPUP as implemented in FSL [18].

2.4.2. Study of grey matter

Abnormal tissues were delineated on the T1-weighed images using MRIcroN for each patient [19]. T1-weighted images were normalized in the Montreal Neurological Institute (MNI) space (http://www.mni.mcgill.ca/) using rigid and elastic deformation tools provided in the software package Statistical Parametric Mapping 8 (SPM8, http://www.fil.ion.ucl.ac.uk/spm). Deformation was applied to the whole brain except for the voxels contained in the lesion mask, in order to avoid deformation of the lesioned tissue [20]. Finally, the lesion was carefully drawn in the MNI space by an expert neuropsychologist (ML) and checked by an expert neurologist (RM). Subsequently, lesions were overlapped for each of the high-responders and low-responders group.

2.4.3. Cortical Thickness preprocessing

Cortical thickness was derived from the T1-weighted imaging dataset using a registration-based method (Diffeomorphic Registration based Cortical Thickness, DiReCT) [21] optimised for patients with a brain lesion in BCBtoolkit (http://toolkit.bcblab.com) [22]. This approach has good scan-rescan repeatability and good neurobiological validity, as it can predict with a high statistical power the age and gender of the participants [23]. These data were then normalized to MNI space with the previous deformation estimated to normalize the T1-weighted imaging dataset.

2.4.4. Study of white matter

We extracted brain using BET implemented in FSL and we corrected diffusion datasets simultaneously for motion and geometrical distortions by using ExploreDTI

(http://www.exploredti.com) [24] . The tensor model was fitted to the data by using the Levenberg-Marquardt non-linear regression [25] .

A fractional anisotropy (FA) map was extracted for each subject by using the function "extract stuff", which is part of the ExploreDTI software package. FA maps were further processed using Tract-Based-Spatial Statistics (TBSS) implemented in FSL (http://fsl.fmrib.ox.ac.uk/fsl/fslwiki/TBSS) [26] , taking in consideration a mask of the damage tissues as in [6] . Next, an average FA map was created and a skeleton map representing the centre of the white matter (FA > 0.2) common to all patients computed. Finally, the registered FA maps were projected into the skeleton.

2.4.5. Statistical analysis

We statistically compared FA and cortical thickness values between low-responder and high-responder patients. Visual field defects and lesion volume were included as co-variables of non-interest. Lesioned voxels were excluded from these analyses. We used the FSL function "Randomise" (http://fsl.fmrib.ox.ac.uk/fsl/fslwiki/Randomise/), with 5,000 random permutation tests and a Threshold-Free Cluster Enhancement option. Results were adjusted for family wise error (FWE) corrections for multiple comparisons and thresholded at $p<0.05$. In addition, we applied the same analyses to explore potential between-group differences in mean diffusivity, axial diffusivity and radial diffusion.

To assess the dimensional relationships between FA, cortical thickness and prism-induced changes in performance, we conducted a regression analysis including all the 14 patients. Lesion volume and visual field defect were included as continuous co-variables of non-interest. We again used the FSL function "Randomise", with 5,000 random permutation tests and a Threshold-Free Cluster Enhancement option. Results were adjusted for FWE corrections for multiple comparisons and thresholded at $p<0.05$. We used BCBtoolkit to further

characterise the white matter tracts passing through the voxels showing a significant difference. For each statistical analysis, effect sizes were calculated using G*power (http://www.gpower.hhu.de/en.html).

2.5. Data Availability Statement

The data are available upon request to the corresponding author.

3. Results

3.1. Behavioral results

Patients demonstrated a relatively stable level of performance before PA; there was no difference between neglect scores assessed one day and two hours before PA (first session: mean score 29.08, SD 20.33; second session: mean score 30.81, SD 21.57; Wilcoxon Signed-Ranks Test, Z=-0.345, p=0.73). PA induced a sensorimotor adaptation in all patients, who deviated rightward before PA (6.47 degrees; SD, 3.51), but leftward after PA (-1.95 degrees; SD, 2.83; Z=-3.234, p=0.001). There was no correlation between neglect recovery scores and PA effect on the straight-ahead task, consistent with previous results [26,27] .

High-responder and low-responder patients had similar age (Mann-Whitney U=34; p=0.23), with high-responders being numerically older (mean, 69.62 years, SD 6.82) than low-responders (59.50 years, SD 13.47). Low-responders had numerically larger lesion volumes, but the difference was not significant (U=14; p=0.23). Low- and high-responders had similar neglect severity scores before PA (U=28; p=0.66). However, high-responders had a shorter delay from stroke (mean number of days from stroke, 341.38; SD, 340.58; range 107-1119) than low-responders (mean, 816.33 days; SD, 484; range 319-1497; U=42, p=0.02). Homonymous hemianopia was present in three low-responders and in three high-responders.

By definition, high-responder patients demonstrated a statistically reliable neglect improvement after PA (Wilcoxon Signed-Ranks Test, Z=-2.52; p=0.012), while this was not the case for the low-responder subgroup (Z=-0.67; p=0.50). In particular, high-responders detected more left items in letter cancellation (Z=-2.39, p=0.017), drew more left-sided items in landscape copy (Z=-2.06, p=0.039) and in daisy drawing (Z=-2.24; p=0.025), and had a more symmetrical performance when bisecting lines (Z=-2.240; p=0.025). However, PA did not significantly impact performance on tasks with minimal motor component, such as the reading task (Z=-1.604; p=0.11) and the Landmark task (Z=-0.365; p=0.715).

3.2. Lesion analysis

The maximum lesion overlap was centered in the right fronto-parietal white matter in both patient subgroups (Figure 1.1). In low-responders, damage also involved the supramarginal and angular gyri of the inferior parietal lobule. Lesion subtraction (Figure 1.2) between low and high responders mostly revealed parietal regions, including the inferior parietal lobule, the postcentral gyrus, but also frontal regions such as the precentral gyrus, the superior frontal lobe, the orbito-frontal cortex, and the fronto-parietal white matter.

3.3. Cortical thickness

A regression analysis between cortical thickness and recovery scores revealed three significant clusters in the left, undamaged hemisphere (Figure 2.1 and Table 2). The first cluster (p=0.037) involved the perisylvian region, including the surface of the inferior parietal lobule, the three temporal gyri, somatosensory areas and the prefrontal cortex, with a medium effect size (0.26). The second cluster (p=0.048) was located in the posterior part of the superior temporal sulcus.

The third cluster (p=0.049) was situated in the anterior portion of the left inferior temporal sulcus. All the clusters had large effect sizes (>0.60).

Controls and high responders had similar values of cortical thickness; low responders had instead lower values in cluster 3 (mean, 0.73) compared with high-responders (2.17) (t=3.9751, df=12, Benjamini-Hochberg-corrected p<0.01), and with controls (mean=2.52) (t=9.48; df=14; Benjamini-Hochberg-corrected p<0.01) (Figure 2.2). There were statistical trends for differences in the same direction in cluster 2 between low-responders and high-responders (means, 0.91 and 1.55, respectively; t=2.51; df=12; Benjamini-Hochberg-corrected p = 0.082), and between low-responders and controls (controls' mean, 1.47; t=2.88; df=14; Benjamini-Hochberg-corrected p=0.055).

3.4. White matter analyses

TBSS showed that low-responders had decreased FA as compared with high-responders in three clusters, all with large effect sizes (>0.80; Figure 3.1, Table 3). The first cluster (p = 0.019) was located in the body of the corpus callosum. The second cluster (p = 0.049) encompassed the genu of the corpus callosum. The third cluster (p = 0.049) was localized in a portion of the genu of the corpus callosum within the left, undamaged hemisphere.

We used BCBtoolkit to visualize the white matter tracts passing through the voxels showing a significant difference between the patient subgroups. The analysis revealed that the fibres intersecting the first cluster mostly connected sensorimotor areas (Figure 3.2). Additional regions in the temporal lobe (middle and superior gyri), and in the parietal lobe (supramarginal gyrus, precuneus and superior parietal lobule) were also involved. The second and the third clusters mostly connected prefrontal areas. The groups did not differ in mean, axial and radial

diffusivity. Regression analyses between FA values and percentage of improvement after PA did not disclose any significant correlations.

A region of interest approach based on the clusters identified by TBSS analysis in patients was used to extract FA values from the ten age- and education-matched healthy participants. Benjamini-Hochberg-corrected comparisons showed similar FA values in high-responders and controls in cluster 1 ($p=0.30$). Low-responders had lower FA values than both controls and high-responders in cluster 1 (all $p<0.01$) and 2 (all $p<0.01$). High- and low-responders had lower FA values than controls in cluster 3 ($p<0.01$), with a tendency for lower FA values for low-responders than for high-responders ($p= 0.081$).

Cortical thickness in clusters 2 and 3 correlated with the 3 clusters of FA values (Table 4), thus suggesting a link between decreased cortical thickness and white matter degeneration. All FA and Cortical thickness clusters were negatively correlated with the delay post-stroke (Table 5).

4. Discussion

In this study, we followed up a group of patients with chronic visual neglect, before and after prism adaptation. The time elapsed from stroke resulted to be shorter in high-responders than in low-responders, which suggests the opportunity to administer PA therapy as soon as possible after the stroke. We used advanced neuroimaging techniques to identify the anatomical predictors of neglect patients' response to PA. First, cortical thickness analyses indicated a significant contribution of the left, undamaged hemisphere. Second, diffusion weighted imaging demonstrated an important role for inter-hemispheric connections in PA efficiency.

In the left, healthy hemisphere, cortical thickness analyses revealed a significant involvement of the temporo-parietal areas in the PA cognitive effect. These regions match areas contributing to right visual neglect after a stroke in the left hemisphere [28] , and mirror classical areas reported as involved in left visual neglect after a stroke in the right hemisphere [28] . This

may suggest that the left temporo-parietal junction is able to compensate for left visual neglect [29] . Consistent with this hypothesis, previous studies reported an involvement of the left hemisphere in the recovery of neglect after PA therapy [9,12] . In healthy individuals, rightward PA increased BOLD response in the left inferior parietal cortex [30] . Our cortical thickness and diffusion results suggest an implication of left prefrontal cortex in prism-induced neglect compensation, consistent with the observation that effective PA in neglect is facilitated by TMS-based disinhibition of the left motor cortex [31] . Altogether, these findings fit well with the fronto-parietal organization of attention networks in the primate brain [32] .

Two possibilities can explain the difference in cortical thickness in the contralesional hemisphere. Some individual brains might have a better predisposition to recover than others (e.g., thanks to a thicker left temporo-parietal junction). This possibility would be consistent with the analogous results obtained in the domain of recovery from aphasia, which appears to be promoted by stronger language structures in the right hemisphere [33,34] . An alternative hypothesis might be that diaschisis and disconnection may have induced secondary atrophy in remote cortices [22,35] . This would be consistent with previous reports suggesting that bilateral diffuse tissue loss may occur in individuals with chronic stroke [36] . Thus, premorbid atrophy in left temporo-parietal areas might hamper cognitive effects related to PA after a stroke in the right hemisphere (see [37]) . Future longitudinal studies comparing acute to chronic stages of vascular strokes may adjudicate between these possibilities.

Our results also showed that low-responder patients had a selective decrease of callosal FA in the body and genu of the corpus callosum, which mainly connect sensorimotor and prefrontal areas [38] . Analysis of other metrics of white matter integrity (RD, MD, AD) in clusters identified by TBSS was consistent with the FA results. Martin-Arévalo et al (2016) [39] showed that leftward PA alters transcallosal motor inhibition between the two motor cortices in the healthy brain, thus confirming the possibility that PA modulates inter-hemispheric interactions.

This result suggests that PA improves left neglect by allowing left-hemisphere attentional networks to access information processed by the lesioned right hemisphere, through the callosal body and genu. An implication of prefrontal circuits in neglect compensation has been hypothesized on the basis of behavioral evidence [40], and recently confirmed by electrophysiological measures [41]. Also consistent with our results, cathodal transcranial direct current stimulation applied over the left posterior parietal cortex interfered with the beneficial effect of PA on neglect [42].

Limitations of the study

We were able to include 14 chronic neglect patients for follow-up before and after PA; the design of the study required this sample to be further subdivided in two subgroups (high- and low-responders). The limited number of inclusions is representative of the difficulties of organizing a longitudinal study of patients with stable neuropsychological deficits, with the associated need of administering lengthy MRI sequences and repeated cognitive assessments. In the present study, five additional neglect patients had to be excluded because they did not tolerate the 1-hour-long neuroimaging procedure used in this study. Despite this limitation, however, the sample size was sufficient to obtain significant results with TBSS, which is a notoriously conservative technique. Also, a power analysis indicated medium to large effect sizes for the left temporo-parietal junction, temporal lobe and white matter findings. Finally, the present anatomical evidence is consistent with previous studies, showing that lesions to the right hemisphere posterior parietal cortex and the superior frontal gyrus [11], the infero-posterior parietal cortex [9], the intra-parietal sulcus, the white matter around the inferior parietal lobule, the middle frontal gyrus [43], the occipital lobe [44] and the right cerebellum (patient 5 in Ref. [12]) hampered PA efficiency. Thus, our patient population appears to be representative of the general lesional patterns in chronic neglect patients.

Summary/Conclusions

Our results confirm the importance for recovery from neglect of the left, healthy hemisphere [29], as well as of efficient inter-hemispheric connections [6]. Specifically, left hemisphere regions homologues to the fronto-parietal attention networks in the right hemisphere [4], as well as callosal pathways passing through the body and the genu, appear to be critical for compensation of neglect signs after a single PA session. It remains to be seen whether or not similar anatomical constraints apply to more prolonged rehabilitation programmes using PA [45]. The identification of anatomical predictors of response to different, labour-intensive rehabilitation strategies may ultimately enable clinicians to select and tailor the appropriate treatment to the specific needs of the individual patient. Even in chronic patients at more than 3 months from the stroke, early administration of PA could be important to improve patients' response. Finally, the relationship between recovery and contralesional cortical thickness suggests potential targets for future therapeutic interventions.

Acknowledgments

We would like to thank Cécile Coste, Fanny Lagneau, Karynne Moreau, Emilie Monnot and Marika Urbanski for patient referral.

Sources of Funding

The research leading to these results has received funding from a CIFRE PhD fellowship to ML, from the ANR "Phenotypes" ANR-13-JSV4-0001-01 to MTS and from the programs "Investissements d'Avenir" ANR-10-IAIHU-06, ANR-10-LABX-0087 IEC and ANR-10-IDEX-0001-002-PSL*.

Disclosure: None

References

1. Mesulam M-M. Principles of Behavioral Neurology. Davis; 1985.
2. Azouvi P, Samuel C, Louis-Dreyfus A, et al. Sensitivity of clinical and behavioural tests of spatial neglect after right hemisphere stroke. J Neurol Neurosurg Psychiatry. 2002;73:160–166.
3. Doricchi F, Thiebaut de Schotten M, Tomaiuolo F, Bartolomeo P. White matter (dis)connections and gray matter (dys)functions in visual neglect: gaining insights into the brain networks of spatial awareness. Cortex. 2008;44:983–995.
4. Corbetta M, Shulman GL. Spatial neglect and attention networks. Annu Rev Neurosci. 2011;34:569–599.
5. Bartolomeo P, Thiebaut de Schotten M, Doricchi F. Left unilateral neglect as a disconnection syndrome. Cereb Cortex. 2007;17:2479–2490.
6. Lunven M, Thiebaut De Schotten M, Bourlon C, et al. White matter lesional predictors of chronic visual neglect: a longitudinal study. Brain. 2015;138:746–760.
7. Yang NYH, Zhou D, Chung RCK, Li-Tsang CWP, Fong KNK. Rehabilitation Interventions for Unilateral Neglect after Stroke: A Systematic Review from 1997 through 2012. Front Hum Neurosci. 2013;7:187.
8. Rossetti Y, Rode G, Pisella L, et al. Prism adaptation to a rightward optical deviation rehabilitates left hemispatial neglect. Nature. 1998;395:166–169.
9. Luauté J, Michel C, Rode G, et al. Functional anatomy of the therapeutic effects of prism adaptation on left neglect. Neurology. 2006;66:1859–1867.
10. Rode G, Lacour S, Jacquin-Courtois S, et al. Long-term sensorimotor and therapeutical effects of a mild regime of prism adaptation in spatial neglect. A double-blind RCT essay. Ann Phys Rehabil Med. 2015;58:40–53.
11. Rousseaux M, Bernati T, Saj A, Kozlowski O. Ineffectiveness of prism adaptation on

spatial neglect signs. Stroke. 2006;37:542–543.

12. Saj A, Cojan Y, Vocat R, Luauté J, Vuilleumier P. Prism adaptation enhances activity of intact fronto-parietal areas in both hemispheres in neglect patients. Cortex. 2013;49:107–119.

13. Barrett AM, Goedert KM, Basso JC. Prism adaptation for spatial neglect after stroke: translational practice gaps. Nat Rev Neurol. 2012;8:567–577.

14. Gainotti G, D'Erme P, de Bonis C. [Clinical aspects and mechanisms of visual-spatial neglect]. Rev Neurol (Paris). 1989;145:626–634.

15. Harvey M, Milner AD. Residual perceptual distortion in "recovered" hemispatial neglect. Neuropsychologia. 1999;37:745–750.

16. Cockcroft DW. Direct challenge tests: Airway hyperresponsiveness in asthma: its measurement and clinical significance. Chest. 2010;138:18S–24S.

17. Andersson JLR, Skare S, Ashburner J. How to correct susceptibility distortions in spin-echo echo-planar images: application to diffusion tensor imaging. NeuroImage. 2003;20:870–888.

18. Smith SM, Jenkinson M, Woolrich MW, et al. Advances in functional and structural MR image analysis and implementation as FSL. NeuroImage. 2004;23, Supplement 1:S208–S219.

19. Rorden C, Brett M. Stereotaxic display of brain lesions. Behav Neurol. 2000;12:191–200.

20. Brett M, Leff AP, Rorden C, Ashburner J. Spatial normalization of brain images with focal lesions using cost function masking. NeuroImage. 2001;14:486–500.

21. Das SR, Avants BB, Grossman M, Gee JC. Registration based cortical thickness measurement. NeuroImage. 2009;45:867–879.

22. Foulon C, Cerliani L, Kinkingnéhun S, et al. Advanced lesion symptom mapping

analyses and implementation as BCBtoolkit. GigaScience. 2018;7:1–17.

23. Tustison NJ, Cook PA, Klein A, et al. Large-scale evaluation of ANTs and FreeSurfer cortical thickness measurements. NeuroImage. 2014;99:166–179.

24. Leemans A, Jones DK. The B-matrix must be rotated when correcting for subject motion in DTI data. Magn Reson Med. 2009;61:1336–1349.

25. Marquardt DW. An Algorithm for Least-Squares Estimation of Nonlinear Parameters. J Soc Ind Appl Math. 1963;11:431–441.

26. Smith SM, Jenkinson M, Johansen-Berg H, et al. Tract-based spatial statistics: voxelwise analysis of multi-subject diffusion data. NeuroImage. 2006;31:1487–1505.

27. Pisella L, Rode G, Farnè A, Boisson D, Rossetti Y. Dissociated long lasting improvements of straight-ahead pointing and line bisection tasks in two hemineglect patients. Neuropsychologia. 2002;40:327–334.

28. Beume L-A, Martin M, Kaller CP, et al. Visual neglect after left-hemispheric lesions: a voxel-based lesion–symptom mapping study in 121 acute stroke patients. Exp Brain Res. Epub 2016 Sep 16.:1–13.

29. Bartolomeo P, Thiebaut de Schotten M. Let thy left brain know what thy right brain doeth: Inter-hemispheric compensation of functional deficits after brain damage. Neuropsychologia. 2016;93:407–412.

30. Tissieres I, Fornari E, Clarke S, Crottaz-Herbette S. Supramodal effect of rightward prismatic adaptation on spatial representations within the ventral attentional system. Brain Struct Funct. Epub 2017 Nov 18.

31. O'Shea J, Revol P, Cousijn H, et al. Induced sensorimotor cortex plasticity remediates chronic treatment-resistant visual neglect. eLife. 2017;6.

32. Lunven M, Bartolomeo P. Attention and spatial cognition: Neural and anatomical substrates of visual neglect. Ann Phys Rehabil Med. 2017;60:124–129.

33. Xing S, Lacey EH, Skipper-Kallal LM, et al. Right hemisphere grey matter structure and language outcomes in chronic left hemisphere stroke. Brain J Neurol. 2016;139:227–241.

34. Forkel SJ, Thiebaut de Schotten M, Dell'Acqua F, et al. Anatomical predictors of aphasia recovery: a tractography study of bilateral perisylvian language networks. Brain J Neurol. 2014;137:2027–2039.

35. Cheng B, Schulz R, Bönstrup M, et al. Structural plasticity of remote cortical brain regions is determined by connectivity to the primary lesion in subcortical stroke. J Cereb Blood Flow Metab. 2015;35:1507–1514.

36. Gauthier LV, Taub E, Mark VW, Barghi A, Uswatte G. Atrophy of spared gray matter tissue predicts poorer motor recovery and rehabilitation response in chronic stroke. Stroke. 2012;43:453–457.

37. Levine DN, Warach JD, Benowitz L, Calvanio R. Left spatial neglect: effects of lesion size and premorbid brain atrophy on severity and recovery following right cerebral infarction. Neurology. 1986;36:362–366.

38. Catani M, Dell'Acqua F, Bizzi A, et al. Beyond cortical localization in clinico-anatomical correlation. Cortex. 2012;48:1262–1287.

39. Martín-Arévalo E, Laube I, Koun E, Farnè A, Reilly KT, Pisella L. Prism Adaptation Alters Electrophysiological Markers of Attentional Processes in the Healthy Brain. J Neurosci. 2016;36:1019–1030.

40. Bartolomeo P. The novelty effect in recovered hemineglect. Cortex. 1997;33:323–332.

41. Takamura Y, Imanishi M, Osaka M, et al. Intentional gaze shift to neglected space: a compensatory strategy during recovery after unilateral spatial neglect. Brain. Epub 2016 Sep 23.

42. Làdavas E, Giulietti S, Avenanti A, et al. a-tDCS on the ipsilesional parietal cortex

boosts the effects of prism adaptation treatment in neglect. Restor Neurol Neurosci. 2015;33:647–662.

43. Sarri M, Greenwood R, Kalra L, Papps B, Husain M, Driver J. Prism adaptation aftereffects in stroke patients with spatial neglect: pathological effects on subjective straight ahead but not visual open-loop pointing. Neuropsychologia. 2008;46:1069–1080.

44. Serino A, Angeli V, Frassinetti F, Làdavas E. Mechanisms underlying neglect recovery after prism adaptation. Neuropsychologia. 2006;44:1068–1078.

45. Frassinetti F, Angeli V, Meneghello F, Avanzi S, Làdavas E. Long-lasting amelioration of visuospatial neglect by prism adaptation. Brain. 2002;125:608–623.

Table 1: Demographical and clinical characteristics of patients, with their performance on visuospatial tests before and after prism adaptation.

	High-Responder group N=8 mean (SD)		**Low-Responder group** N=6 mean (SD)		
Descriptive data					
Age (years)	69.62 (6.82)		59.5 (13.47)		p=0.230
Education	12.25 (3.65)		12 (2.82)		p=0.895
Lesion volume (cm^3)	106.53 (110,60)		228.98 (183,21)		p=0.230
Lesion-testing delay (days)	341.40 (340.59)		816.33 (484.29)		**p=0.02**
Motor deficit (number of patients)	4		3		
Visual field defect (number of patients)	3		3		
Neuropsychological results					
MMSE	27.00 (1.69)		26.83 (2.40)		p=0.881
Recovery rate (%)	36.29 (15.36)		-1.60 (22.18)		**p<0.01**
	Pre	**Post**	**Pre**	**Post**	
Neglect severity global score (%)	32.38 (20,10)	21.64 (16.69)	32.18 (24.96)	30.72 (19.53)	
Letter cancellation (left omissions)	10.25 (7.63)	4.62 (6.09)	7.83 (11.29)	7.00 (9.63)	
Gainotti drawing (max 6)	4.50 (1.07)	5.20 (1.00)	4.33 (1.21)	4.83 (1.33)	
Reading task (max 116)	8.50 (12.75)	3.00 (3.82)	16.00 (35.78)	16.00 (37.24)	
Line bisection (rightward deviation, mm)	20.08 (22.43)	8.35 (15.87)	16.04 (28.89)	10.23 (25.27)	
Daisy drawing (max 3)	2.00 (0.92)	2.62 (1.06)	1.33 (0.82)	1.50 (0.84)	
Landmark task ("left shorter" answers, max 12)	8.00 (3.78)	7.5 (3.74)	8.00 (3.29)	9.00 (3.29)	

Table 2: Grey matter clusters showing decreased cortical thickness associated with poor recovery after PA therapy

GM clusters	MNI coordinates			CS	Corrected *P*	Effect size *d*
	x	*y*	*z*			
1. L perisylvian regions	-43	-3	-21	31947	0.037	0.26
2. L Temporo-parietal junction	-48	-55	15	1539	0.048	0.67
Angular g						
Middle temporal lobe						
3. L Temporal lobe	-33	-16	-32	670	0.049	1.24
ITg						
L fusiform g						
Parahippocampal g						

CS, cluster size (i.e., number of voxels); L, left; g, gyrus; ITL, inferior temporal gyrus; IPL, inferior parietal lobule.

Grey matter clusters significantly associated with poor recovery of neglect after prism adaptation (P_{TFCE}<0.05). Coordinates indicate the location of the cluster peak in Montreal Neurological Institute (MNI) convention.

Table 3: White matter clusters showing decreased fractional anisotropy FA (P_{TFCE}<0.05) in the low-responder group as compared with the high-responder group

WM clusters	MNI coordinates			CS	Corrected *P*	Effect size *d*
	x	*y*	*z*			
1. CC body	2	-20	24	1533	0.019	1.57
2. CC genu	0	24	0	47	0.049	1
3. L CC genu	-12	31	-2	9	0.049	0.85

CS, cluster size (i.e., number of voxels); CC, corpus callosum; L, left.

Coordinates indicate the location of the cluster peak in Montreal Neurological Institute (MNI) convention.

Table 4: Spearman correlations between the three FA clusters identified in the TBSS analysis and the three cluster identified in the cortical thickness study

	FA Cluster 1	**FA Cluster 2**	**FA Cluster 3**	**CT Cluster 1**	**CT Cluster 2**	**CT Cluster 3**
FA Cluster 1						
FA Cluster 2	**0.855****					
FA Cluster 3	**0.780****	**0.864****				
CT Cluster 1	0.253	0.358	0.437			
CT Cluster 2	**0.582***	**0.692****	**0.705****	**0.873****		
CT Cluster 3	**0.701****	**0.767****	**0.771****	**0.648****	**0.798****	

** $p<0.01$; * $p<0.05$, FA Fractional Anisotropy, CT Cortical Thickness,

Table 5: Spearman correlations between imaging clusters and delay post stroke

	Cluster 1 FA	Cluster 2 FA	Cluster 3 FA	Cluster 1 CT	Cluster 2 CT	Cluster 3 CT
Correlation coefficient with delay post stroke	-0.71**	-0.58*	-0.59*	-0.49*	-0.65**	-0.62**

** $p<0.01$; * $p<0.05$, FA Fractional Anisotropy, CT Cortical Thickness,

Figure legends

Figure 1: Patients' grey matter lesion anatomy. (1) Overlap of the lesions for all the included right brain-damaged patients for each group. (2) Results of the subtraction of the probability map of the high-recovery group from the probability map of the low-recovery group. Maps show the Z-statistics rank order statistics. All peaks are significant at $p<0.05$ level

Figure 2: Cortical thickness analysis. (1) Relationship between cortical thickness and recovery rate score represented by the four clusters. Results are represented at $p<0.05$ and corrected for multiple comparisons. LH, left hemisphere; RH, right hemisphere (2) Comparison of cortical thickness values between the three groups for each cluster identified in the "randomise" analysis

Figure 3: White matter analysis. (1) Results of TBSS between-groups comparisons represented by the three clusters. FA differences ($p<0.05$) are represented in red. **(2)** Percentage maps in healthy subjects (BCB toolkit (http://www.brainconnectivitybehaviour.eu) showing the cortical projections of the voxels identified by TBSS analysis in low recovery patients compared to high-recovery patients.
LH, left hemisphere; RH, right hemisphere.

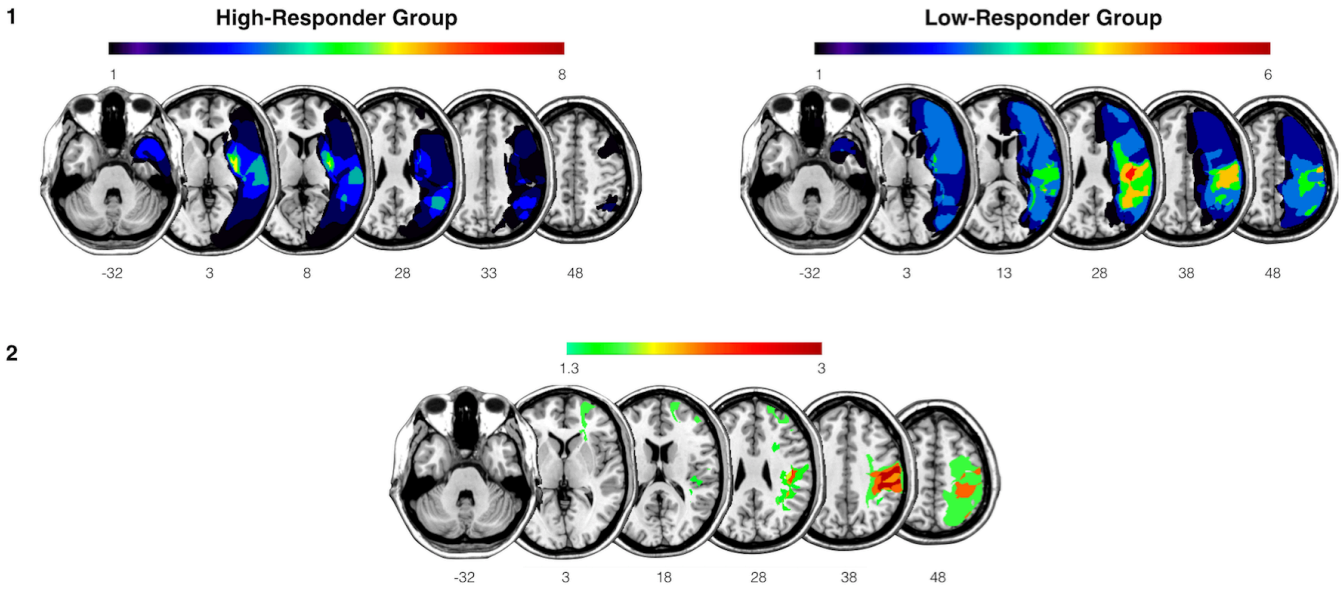
1
High-Responder Group
1
8
-32
3
8
28
33
48
Low-Responder Group
1
6
-32
3
13
28
38
48
2
1.3
3
-32
3
18
28
38
48

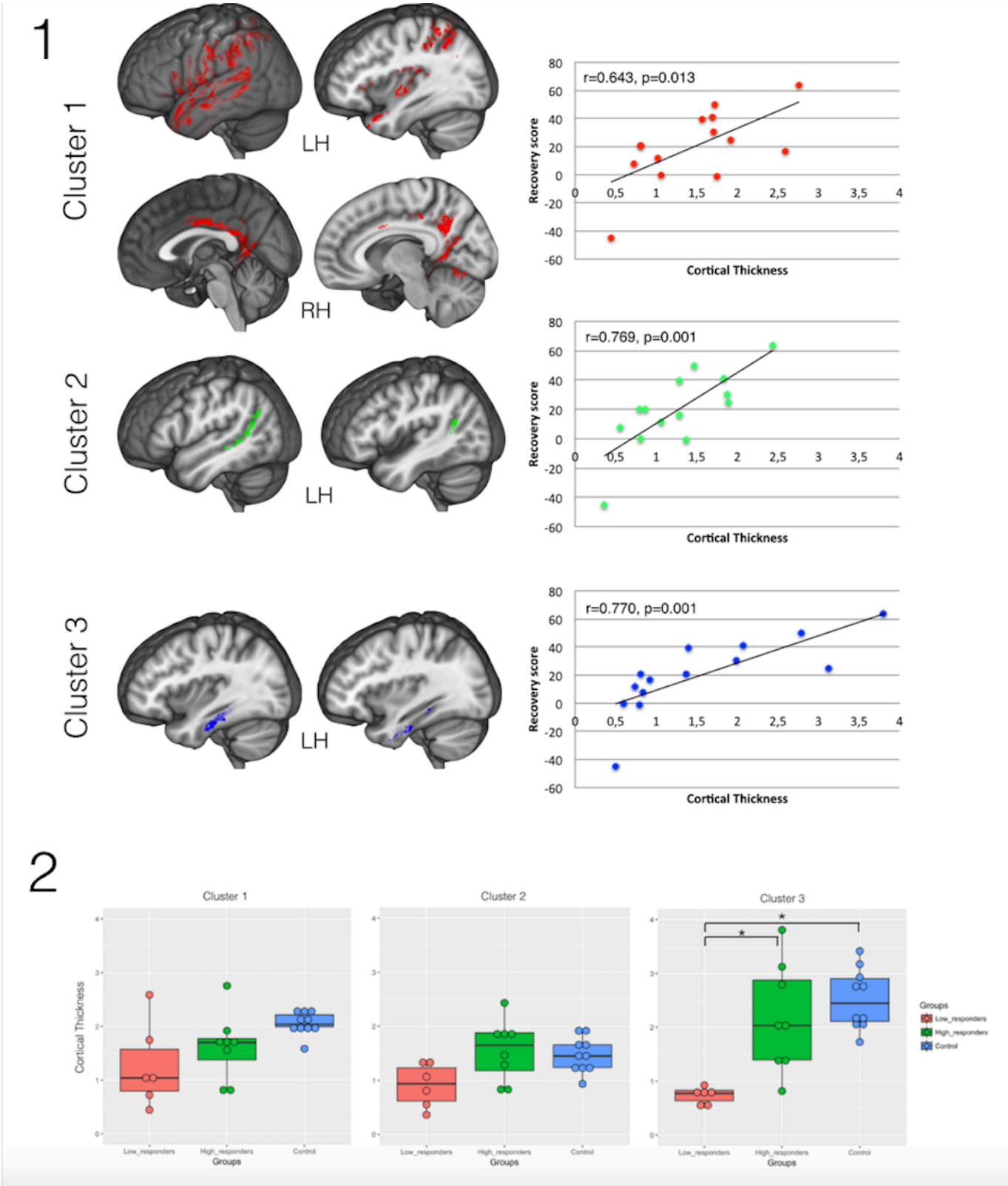
1
Cluster 1
LH
RH
r=0.643, p=0.013
Recovery score
Cortical Thickness
Cluster 2
LH
r=0.769, p=0.001
Recovery score
Cortical Thickness
Cluster 3
LH
r=0.770, p=0.001
Recovery score
Cortical Thickness
2
Cluster 1
Cluster 2
Cluster 3
Cortical Thickness
Low_responders
High_responders
Control
Groups

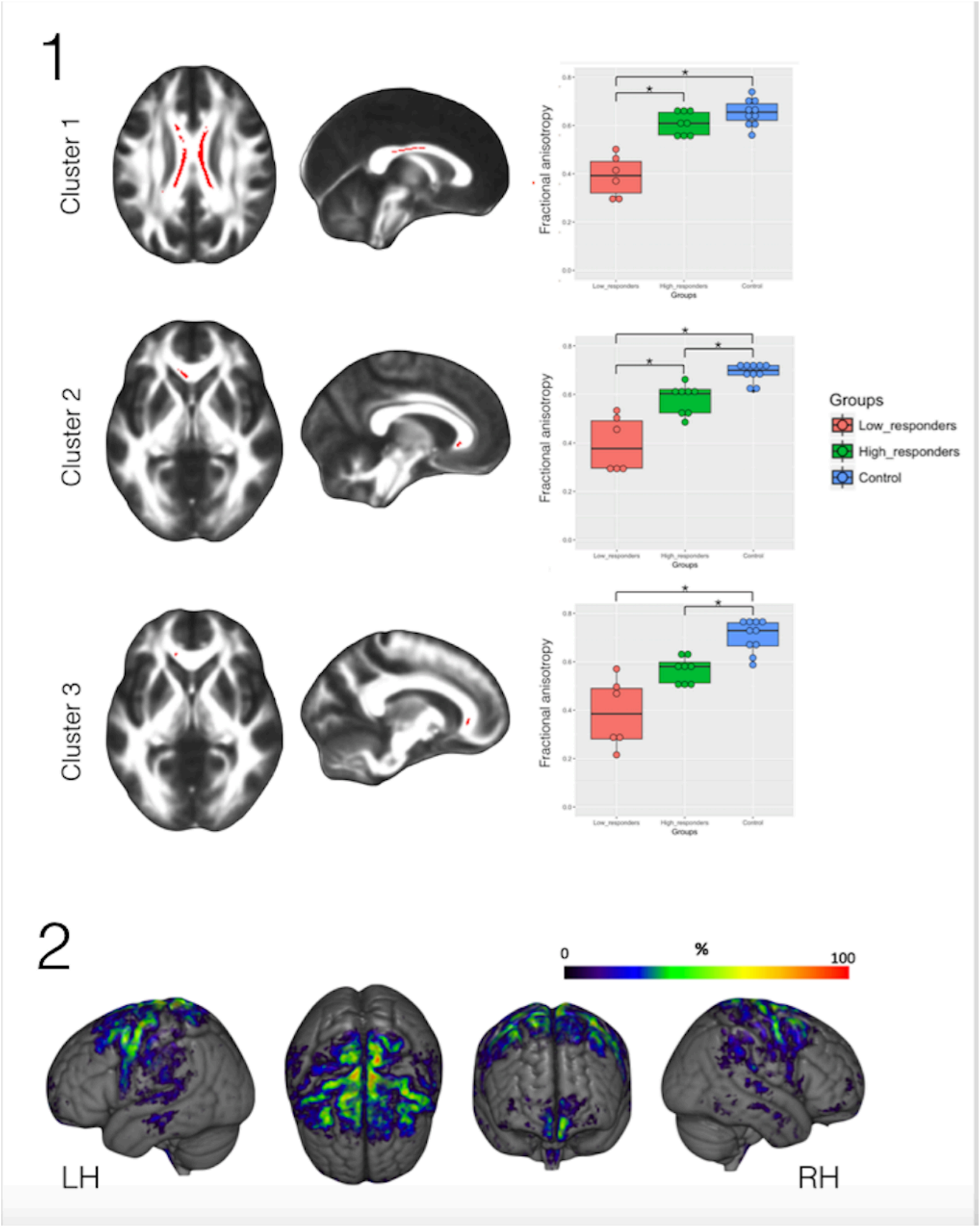
1
Cluster 1
Cluster 2
Cluster 3
Fractional anisotropy
Groups
Low_responders
High_responders
Control
2
0
%
100
LH
RH